molecular pharmaceutics

Article

pubs.acs.org/molecularpharmaceutics

# Dendrimer Nanocarriers for Transport Modulation Across Models of the Pulmonary Epithelium

Balaji Bharatwaj,[†] Abdul Khader Mohammad,[‡] Radovan Dimovski,[†] Fernando L. Cassio,[§] Reinaldo C. Bazito,[§] Denise Conti,[†] Qiang Fu,[‡] Joshua Reineke,[‡] and Sandro R. P. da Rocha*[,†]

[†]Department of Chemical Engineering and Materials Science, and [‡]Department of Pharmaceutical Sciences, Wayne State University, Detroit, Michigan 48202, United States

[§]Department of Chemistry, State University of Sao Paulo, Sao Paulo, Brazil

Supporting Information

**ABSTRACT:** The purpose of this study was to determine the effect of PEGylation on the interaction of poly(amidoamine) (PAMAM) dendrimer nanocarriers (DNCs) with *in vitro* and *in vivo* models of the pulmonary epithelium. Generation-3 PAMAM dendrimers with varying surface densities of PEG 1000 Da were synthesized and characterized. The results revealed that the apical to basolateral transport of DNCs across polarized Calu-3 monolayers increases with an increase in PEG surface density. DNC having the greatest number of PEG groups ($n$ = 25) on their surface traversed at a rate 10-fold greater than its non-PEGylated counterpart, in spite of their larger size. This behavior was attributed to a significant reduction in charge density upon PEGylation. We also observed that PEGylation can be used to modulate cellular internalization. The total uptake of PEG-free DNC into polarized Calu-3 monolayers was 12% (w/w) vs 2% (w/w) for that with 25 PEGs. Polarization is also shown to be of great relevance in studying this *in vitro* model of the lung epithelium. The rate of absorption of DNCs administered to mice lungs increased dramatically when conjugated with 25 PEG groups, thus supporting the *in vitro* results. The exposure obtained for the DNC with 25PEG was determined to be very high, with peak plasma concentrations reaching 5 $\mu g \cdot mL^{-1}$ within 3 h. The combined *in vitro* and *in vivo* results shown here demonstrate that PEGylation can be potentially used to modulate the internalization and transport of DNCs across the pulmonary epithelium. Modified dendrimers thereby may serve as a valuable platform that can be tailored to target the lung tissue for treating local diseases, or the circulation, using the lung as pathway to the bloodstream, for systemic delivery.

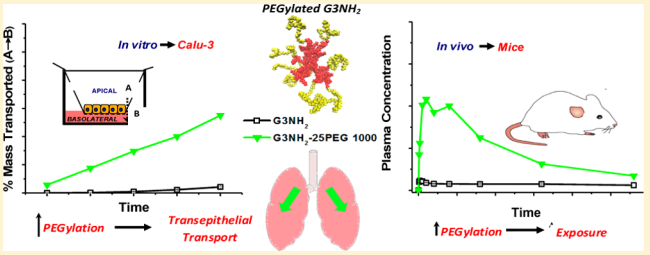


**KEYWORDS:** *respiratory drug delivery, Calu-3, poly(amido amine) dendrimers, PEGylation, in vitro transport, modulation, in vivo pharmacokinetics*

## 1. INTRODUCTION

Oral inhalation (OI) is not only the preferred mode of administration of therapeutics intended for the regional delivery to the lungs, but it has also been recognized as a promising route for the noninvasive delivery of drugs through the lungs,[1,2] as suggested by the many ongoing clinical trials of OI formulations dealing with therapeutics intended for systemic circulation.[3−5] Some of the potential advantages of the OI route include the large surface area, low proteolytic activity, and the thin cellular barrier of the lung tissue, which may be explored to enhance drug bioavailability and transport to bloodstream.[2,6]

Polymeric nanocarriers (PNCs) may be successfully explored in combination with OI formulations for the controlled and targeted local delivery of therapeutics to the lung tissue, and to modulate the transport of drugs across the airway epithelia. Such advancements hold great promise in the delivery of both small molecules and biomacromolecules for the treatment of medically relevant diseases of the lung tissue and systemic ailments alike.[7−13]

The ease in which the size, morphology, and surface chemistry of PNCs can be tailored is perhaps the most attractive feature of such drug carriers. These properties can be used to modulate the interaction of the nanocarriers with intra- and extracellular barriers so as to selectively target desired cell populations and even specific cellular organelles.[7,14,15] Given such potential advantages, there are tremendous opportunities in combining the development of innovative OI formulations for the regional and systemic delivery of drugs to and through the lungs using PNCs.

Dendrimer nanocarriers (DNCs) represent a particularly interesting class of PNCs as they are especially suited to tackle the many challenges that exist in the development of carriers for the delivery of drugs to and through the lungs. DNCs are

**Received:** October 2, 2014
**Revised:** November 29, 2014
**Accepted:** December 2, 2014
**Published:** December 2, 2014

  

DOI: 10.1021/mp500662z
*Mol. Pharmaceutics* 2015, 12, 826−838

hyperbranched synthetic molecules with high monodispersity and multivalency at the surface that provides for a facile route for the attachment of a range of moieties, including therapeutic and imaging agents.[9,16−18] This surface polyfunctionality can also be potentially exploited to tailor the DNCs with functional groups that can be used to modulate (i) the rate and mechanism of cellular uptake and (ii) the extent of permeation across unyielding extra and intracellular barriers populating the lung epithelium and thus optimize the carrier chemistry for either local or systemic delivery.

The goal of this study was to design DNCs with surface functionalities that would allow us to modulate their interaction with the pulmonary epithelium. Generation 3 (G3) poly(amido amine) (PAMAM) dendrimers with varying surface densities of PEG (MW 1000 Da, $G3NH_2$-nPEG1000) were synthesized, characterized, and their toxicity evaluated on the most widely used model of the airway epithelium: Calu-3 cells. Transport studies of the conjugates were conducted across polarized Calu-3 monolayers. The cellular uptake (rate and amount) was followed by flow cytometry, and the total cellular uptake was quantified using cell lysis, also on polarized monolayers. The relative pharmacokinetic parameters of selected conjugates were investigated upon lung and i.v. delivery to Balb/c mice so as to assess the potential of PEGylation to mediate the transport of the DNCs across an *in vivo* model of the pulmonary epithelium. This represents the first study of the effect of PEGylation of PAMAM DNCs on their cellular internalization and transport across both *in vitro* and *in vivo* relevant models of the pulmonary epithelium.

## 2. MATERIALS

Amine-terminated, generation 3 (G3) poly(amido amine) (PAMAM) dendrimer ($G3NH_2$), with 32 surface groups and 6882 Da as determined by MALDI (mass reported by the vendor is 6909 Da), poly(ethylene glycol) monomethyl ether (mPEG, $M_n$ 1000 Da), 1-ethyl-3-(3-(dimethylamino)propyl) carbodiimide (EDC), *N*-Hydroxysuccinimide (NHS), potassium *tert* butoxide, ethyl bromoacetate, fluorescein isothiocyanate (FITC), Bovine Serum Albumin (BSA), Trypan Blue (0.4%), Trypsin supplemented with 0.25% EDTA (for flow cytometry), osmium tetroxide ($OsO_4$), and Triton-X-100 were all purchased from Sigma (St.Louis, MO) and used as received unless otherwise specified. $G3NH_2$ dendrimers were dried in vacuum for 24 h to remove traces of methanol before the reaction. mPEG was purified by dissolving the raw compound in chloroform and drying the resulting solution over anhydrous magnesium sulfate. The final product was obtained by filtering and then evaporating the sample in a rotavapor. Samples were stored in a desiccator prior to usage. Anhydrous dimethyl sulfoxide (DMSO) was purchased from Acros. Deionized water (DI water) with a resistivity of 18.2 MΩ·cm$^2$ was used in all experiments. Hanks' balanced salt solution (HBSS, 1×) supplemented with 0.01 M (4-(2-hydroxyethyl)-1-piperazineethanesulfonic acid) (HEPES) was prepared according to a procedure detailed elsewhere.[19] Human bronchial epithelial cell line Calu-3 (HTB-55) was purchased from ATCC (Manassas, VA). Tissue culture flasks (Greiner BioOne, 75 cm$^2$), 24 (Corning Costar) and 96 well plates (Greiner BioOne), and Transwell Inserts (#3470, polyester membrane, Corning, 0.33 cm$^2$, 0.4 μm pore size) were all purchased from VWR. Dulbecco's Modified Eagle's Media (DMEM) and trypsin (TRYple express) were obtained from Invitrogen. Fetal Bovine Serum (FBS, nonheat inactivated) was procured from Atlanta Biologicals (Atlanta, GA). Rabbit anti ZO-1 (Mid) antibody, Alexa Fluor 546 goat antirabbit IgG (H+L), and 4′,6-diamidino-2-phenylindole, dilactate (DAPI, dilactate) were purchased from Molecular Probes. All antibodies were diluted 100 times in phosphate buffered saline (5 μg, PBS, pH 7.4), supplemented with 6% (w/v) BSA (to prevent nonspecific binding of the antibody) prior to usage. DPX mounting medium was obtained from Fluka. MTT (3-(4,5-dimethylthiazol-2-yl)-2,5-diphenyltetrazolium bromide) assay was purchased from Life Technologies and was utilized as per the protocol detailed by the manufacturer. BCA protein assay was purchased from Pierce (Evanston, IL). Microscope slides and cover glass slides (18 mm$^2$) were obtained from Fisher. All glassware was washed thoroughly in water and dried under vacuum prior to usage. All other chemicals used were purchased from Fisher and EMD, were of HPLC grade, and used as received, unless otherwise noted. Isoflurane was purchased from VetOne. Heparin sodium salt was purchased from Sigma and dissolved in sterile saline to make a 10 U/mL final concentration.

## 3. METHODS

**3.1. Synthesis and Characterization of Carboxylic Acid-Terminated mPEGs (cmPEG).** cmPEG was synthesized according to a procedure described in the literature. Details are provided in the Supporting Information.

**3.2. Conjugation of PEG Grafts and FITC to G3-$NH_2$.** Conjugation of PEG to G3-$NH_2$ was accomplished by reacting the carboxyl-terminated end of the cmPEG to the amine surface group of $G3NH_2$ via EDC-NHS coupling reaction, in a strategy similar to that reported in the literature.[20] Labeling of FITC to the $G3NH_2$ surface and the PEGylation was done in a one pot synthesis.[21−23] Details are provided in the Supporting Information.

**3.3. Culture of Calu-3 Cells.** Calu-3 cells, derived from human bronchial airway epithelium, between passages 36 and 50, were used as models to study the transport and internalization of dendrimer conjugates. Details of the cell culture procedure are provided in the Supporting Information.

**3.4. Cytotoxicity of $G3NH_2$-nPEG1000 Conjugates.** Cell viability of $G3NH_2$-nPEG1000 conjugates was determined using the MTT assay (Promega) as described in the literature.[24] Details are provided in the Supporting Information.

**3.5. Cell Culture for Transport Studies.** For transport experiments, cells were seeded on the apical compartment of Transwell cell culture supports at a density of $0.5 \times 10^6$ cells·cm$^{-2}$. The inserts were then positioned onto 24 well plates containing 0.6 mL of medium on the basolateral side of the inset. To the apical side, 0.2 mL of culture medium was added. The cells were incubated at 37 °C and 5% $CO_2$ atmosphere and grown in a liquid-covered culture (LCC) for 2 days. The medium in the apical compartment was then removed, and the cells were allowed to grow at an air−interface culture (AIC). The medium in the basolateral compartment was replaced every 2 days, and the cells continued to grow under AIC. Transepithelial electrical resistance (TEER) measurements were conducted using Chopstick electrodes (STX-2) and an EVOM voltohmmeter (World Precision Instruments, Florida) in order to ascertain the monolayer confluence. The apical (where the monolayer is cultured) and the basolateral chambers were fed with appropriate volumes of fresh warmed culture media and the insets were returned to the incubator for equilibration for 30 min. The monolayer resistance was


DOI: 10.1021/mp500662z
*Mol. Pharmaceutics* 2015, 12, 826−838

measured after equilibration, and the true monolayer resistance was calculated by subtracting the EVOM reading of the cell-free culture insert from the reading obtained from cell-laden insert and normalizing for the surface area of the support. The TEER values reported in this study represent the average resistance of monolayers cultured in 16 separate Transwell inserts.

**3.6. Electron Microscopy of Cell Monolayers.** Once the peak TEER values were attained, some of the cell monolayers were subject to scanning electron microscopy (SEM) in order to evaluate their morphological features. The monolayers for SEM were prepared according to a procedure described in the literature.[19] Details are provided in the Supporting Information.

**3.7. Immunocytochemistry.** Immunocytochemistry was performed on confluent Calu-3 monolayers in order to visualize the presence of a tight junctional protein, ZO-1, according to the protocol detailed by the manufacturer.[25] Details are provided in the Supporting Information.

**3.8. Epithelial Permeability of the Dendrimer Conjugates Across Calu-3 Monolayers Seeded in Transwell Inserts.** Transport experiments were conducted once the cell monolayers reached confluence and the TEER values peaked (around day 15). The TEER of the cell monolayers was measured prior to starting the experiments. The culture media in the insets was replaced with warm 1× Hank's balanced salt solution (HBSS) at both the apical and basolateral chambers, and the cells were allowed to equilibrate for 30 min. After that, the HBSS on the side was removed, and replaced with HBSS containing a known molar concentration (25 nmol) of FITC-conjugated $G3NH_2$-nPEG1000 of varying PEG surface density ($n$). In order to maintain sink conditions, the insets were moved to a well containing fresh HBSS (1×) at predetermined times, and a known volume of HBSS from the basolateral side of the spent insert was removed and analyzed for the FITC-conjugated dendrimer using a fluorescence spectrometer (PerkinElmer LS50B) in order to determine the extent of transport of dendrimer from the apical onto the basolateral (A → B) side. The apparent permeability ($P_{app}$) from A → B, which indicates the ease of flow of the dendrimer nanocarriers across the monolayer, was calculated according to eq 1:

$$P_{app} = F/(AC_o) \quad (1)$$

where $F$ is the flux or rate of change of cumulative mass transported, $A$ is the area of the inset, and $C_0$ is the initial concentration of $G3NH_2$-nPEG1000 in the donor (apical) compartment.

Dendrimer-free HBSS incubated on the apical side of the inset was used as control. Recording of TEER was accomplished (as described earlier) at every single time point of basolateral sampling to determine the effect of $G3NH_2$-nPEG1000 incubation on the tight junctions of Calu-3 monolayers. After completion of the experiments, samples from the apical side were removed and stored for further analysis. Select cell monolayers (from each condition) were washed twice with HBSS and were replenished with the growth medium on the apical side to estimate the revival of TEER after completion of the permeability experiments.

For mass balance studies, after each time point, selected inserts were chosen ($n$ = 3 for each conjugate), and the dendrimer-laden buffer in the apical chamber was removed and analyzed to estimate the extent of dendrimer remaining after internalization and transport. The extent of transport of the conjugate onto the basolateral compartment was estimated as mentioned in the earlier part of this section. For quantifying the internalized conjugates, cell monolayers were first washed with cold HBSS to arrest uptake. Subsequently the monolayers were lysed using 2% triton-X-100 overnight, and the lysate was analyzed for the internalized conjugates using fluorometry. The resulting lysate was centrifuged to isolate the cell debris, and the supernatant was analyzed for the FITC-labeled PEGylated dendrimer using fluorometry. The dendrimer uptake was normalized to the cellular protein content using BCA assay, according to the protocol described by the manufacturer.[26] Summation of the mass internalized, mass transported and the mass remaining on the apical side was compared against the initial mass pulsed to obtain the overall mass balance.

The ability of dendrimer nanocarriers to diffuse across mucus was investigated according to methodology reported in the literature,[27] with a few modifications. Transwell insert (polyester tissue culture-treated membrane, 3 $\mu$m pore size,[28] and 0.33 $cm^2$ surface area) was positioned inside the well of a 24 well plate, containing 600 $\mu$L of HBSS 1× pH 7.1 supplemented with 0.01 M HEPES (acceptor side). Dendrimer nanocarriers were mixed with synthetic mucus and 30 $\mu$L (mucus layer ∼900 $\mu$m thick) was pulsed on top of the membrane of the inset (donor side). The plate was incubated at 37 °C, and at specific time points, the inset was moved to a new well containing fresh HBSS-HEPES buffer. To quantify the extent of dendrimer diffusing across the mucus (from donor to acceptor side) a known volume was removed from the acceptor side, and the fluorescence of FITC-conjugated dendrimer was measured by using a BioTek Synergy 2 Microplate Reader. Regular synthetic mucus[29] was prepared by mixing mucin (23 $mg.mL^{-1}$) with mucus buffer (85 mM NaCl, 20 mM HEPES, pH 7.4) overnight at 4 °C.[30] Experiments were performed in triplicate.

**3.9. Cellular Internalization of the Dendrimer Nanocarriers in Polarized Calu-3 Cell Monolayers.** Cellular internalization experiments using flow cytometry were conducted on polarized Calu-3 monolayers. Calu-3 cells were plated at a density of $1 \times 10^6$ cells per well in a 24-well plate in DMEM as described in earlier sections and allowed to proliferate to confluence for a period of 8−10 days, with the monolayer periodically checked for confluence by staining the cells for tight junctional protein, ZO-1, and ascertaining its presence through fluorescence microscopy. Once the monolayer integrity was confirmed, the cells were subject to uptake studies. Prior to commencing internalization studies, the cells were incubated for a period of 30 min in warm 1× HBSS. This was followed by incubating the acclimatized monolayers of Calu-3 with 25 nmol of $G3NH_2$-nPEG1000 (in 0.5 mL HBSS) of varying surface densities of PEG, for varying durations (5, 4, 3, 2, 1, 0.5, and 0.25 h). After lapse of the incubation period, the conjugate laden media was carefully aspirated, and the cell monolayers were washed thrice with cold HBSS. The extracellular fluorescence was quenched using 0.2% Trypan Blue, washed again with HBSS, and the cells trypsinized (trypsin supplemented with 0.25% EDTA) and subjected to centrifugation (1200 rpm, 6 min) to recover the cell pellet. The cell pellet thus recovered was resuspended in 1 mL of fresh 1× HBSS and subjected to flow cytometry (BD LSR II, BD Biosciences, San Jose, CA) with a coherent sapphire laser (488 nm) and detected through a 530/30 bandpass filter (FITC). For analysis, at least 6000 events were counted, only viable cells were gated for fluorescence analysis, and 1× HBSS was used as controls for the conjugates. The extent and rate of cellular entry was determined by plotting the mean fluorescence intensity


DOI: 10.1021/mp500662z
Mol. Pharmaceutics 2015, 12, 826−838

Table 1. Number of PEG Grafts ($n$), MW, Size (Diameter), and Zeta Potential ($\zeta$) for the FITC-Modified $G3NH_2$-nPEG1000 Conjugates as Determined by $^1$H-NMR, MALDI, and Light Scattering (LS); LS Measurements Were Conducted in HBSS (pH 7.4) and Room Temperature

| | NMR | | MALDI | | | | |
|---|---|---|---|---|---|---|---|
| compd | $n_{PEG}$[a] | MW | $n_{PEG}$[b] | MW[b] | size ± SD[d] (nm) | $\zeta$ ± SD[d] (mV) | $n_{FITC}$[e] |
| $G3NH_2$ | 0 | 6909[c] | 0 | 6882 | 2.9 ± 1.0 | +21.0 ± 4.8 | 0 |
| $G3NH_2$-0PEG1000 | 0 | 8076 | 0 | 7660 | 3.6 ± 0.5 | +15.5 ± 5.3 | 2.0 |
| $G3NH_2$-5PEG1000 | 5 | 13805 | 4 | 11403 | 4.8 ± 0.9 | +1.1 ± 0.4 | 1.5 |
| $G3NH_2$-13PEG1000 | 13 | 23586 | 9 | 18160 | 5.5 ± 1.4 | −1.4 ± 0.8 | 1.7 |
| $G3NH_2$-25PEG1000 | 25 | 38267 | 23 | 34015 | 7.9 ± 1.0 | −4.7 ± 1.2 | 2.0 |

[a]Average $n_{PEG}$ units conjugated per PAMAM molecule, estimated from the $^1$H NMR spectra of the compound in DMSO-$d_6$. [b]Estimated from the MALDI MW distribution using DHB as matrix, using FlexAnalysis software. [c]Provided by the manufacturer. [d]Four repeats. [e]As determined by $^1$H NMR.

(MFI) values as a function of time. The results reported here are averages of 6 wells for each conjugate.

**3.10. *In Vivo* Transport Studies.** All animal experiments were conducted in accordance to the Institutional Animal Care and Use Committee at Wayne State University. Seven week old, male Balb/c mice weighing between 20 and 25 g were purchased from Charles River, Inc. All animals were allowed to acclimatize for a week prior to experimentation and were housed in a pathogen free environment in HEPA filtered cages. Animals had access to food and water *ad libitum*.

Pulmonary administration of the $G3NH_2$-nPEG1000 of varying surface densities of PEG 1000 Da was performed using the pharyngeal aspiration (PA) technique. Briefly, the mice were anesthetized by inhalation of 2.5% v/v isoflurane and placed on a slant board with the back resting on the board and partially suspended with a rubber band by their incisors. The tongue was held gently in extension and the $G3NH_2$-nPEG1000 solution was placed in the pharynx region by means of a microsyringe. The tongue was continuously held in extension until several breaths had elapsed. Once the entire dosage (100 $\mu$L) was administered, the mice were returned to their housing and monitored for rapid recovery. This method has been validated in comparison to intratracheal administration, and allows for greater lung deposition and higher dose−dose consistency.[31] For intravenous (i.v.) administration, 100 $\mu$L of the $G3NH_2$-nPEG1000 solution was injected into the tail vein. The solutions of $G3NH_2$-nPEG1000 were prepared in sterile normal saline, and a dose of 200 $\mu$g (in 100 $\mu$L) was given to all study groups.

*3.10.1. Blood Sampling and Lung Harvesting.* After administration of the solution of $G3NH_2$-nPEG1000 to mice (i.v. and PA), blood samples were collected at predetermined time points (0.5, 1, 3, 6, 12, 24, 48, and 96 h, and then at 1, 2, 3, and 4 weeks) from each animal. At each time point, 60 $\mu$L of blood was extracted via the tail vein into tubes containing 20 $\mu$L of heparin. The blood sample was centrifuged at 5000 rpm for 30 s, and plasma was collected. Plasma sampled was analyzed for FITC fluorescence (Synergy, BioTek Instruments) and the $G3NH_2$-nPEG1000 was determined by comparing the fluorescence values to a previously prepared calibration curve constructed using the FITC-conjugated $G3NH_2$-nPEG1000. Whole lung tissues were homogenized, followed by extraction with 3 N sodium hydroxide for a period of 72 h in darkness. This procedure dissolved the tissue elements after which the contents were centrifuged to rid the sample of undissolved proteins. The clear supernatant obtained was separated and analyzed for FITC fluorescence. The resulting fluorescence data was compared against standard curves generated by adding known amounts of each $G3NH_2$-nPEG1000 to untreated lung homogenates that were processed concomitantly to determine total residual mass of $G3NH_2$-nPEG1000 within the lungs.[8]

*3.10.2. Pharmacokinetic (PK) Analysis.* Pharmacokinetic analysis was carried out with WinNonlin 5.2, using non-compartmental analysis with two models: i.v. bolus for data collected following i.v. administration and extravascular for the data collected following pulmonary administration (PA). Parameters calculated include the absorption rate constant ($K_a$), clearance ($Cl$), elimination rate constant ($K_{el}$), the elimination half-life ($T_{1/2}$), peak in plasma concentration after drug administration ($C_{max}$), time to reach $C_{max}$ ($T_{max}$), and area under the curve (AUC).

**3.11. Statistical Analysis.** Statistical analysis of the data was performed by two-way ANOVA followed by Tukey's posthoc analysis using OriginPro (v9.0, OriginLab) and SAS. Probability values of $P < 0.05$ were deemed significant. Results reported as mean ± SD (standard deviation).

## 4. RESULTS AND DISCUSSION

**4.1. Synthesis and Characterization of FITC-Labeled $G3NH_2$-nPEG1000.** There are many potential advantages in PEGylating dendrimer nanocarriers for drug delivery applications. The literature shows that PEGylation reduces the cytoxicity of amine-terminated PAMAM.[16] PEGylation also improves the aqueous solubility of dendrimers,[32] which is particularly relevant when conjugating hydrophobic therapeutics to the carriers; otherwise, the carrier−conjugate systems may become completely insoluble. Further, PEGylation has been shown to enhance circulation times of nanocarriers upon systemic administration.[33] PEGylation of nanocarriers can also potentially favor their transport across extracellular barriers of the respiratory epithelium, as PEG reduces the interaction between the carrier and the mucus lining of the airways and the surface fluid of the alveolar region. It is important to note that this has been demonstrated for solid nanoparticles (much larger in size than dendrimers) but has not been established for DNCs.[14]

FITC-labeled $G3NH_2$, with varying surface densities of PEG1000 ($G3NH_2$-nPEG1000), were synthesized as described in detail in the Supporting Information. The resulting products were characterized by MALDI and $^1$H NMR; spectra are also provided in the Supporting Information. A summary of the conjugates synthesized in this work, along with their characteristics, including the number of PEG1000 and FITC grafts, their MW, size, and surface charge is provided in Table 1.

While the numbers estimated by NMR and MALDI are similar, it is interesting to note that there is an underestimation


DOI: 10.1021/mp500662z
Mol. Pharmaceutics 2015, 12, 826−838

of the MW (ca. 10−15%) in the case of MALDI, when compared to that of NMR. This behavior is similar to that observed in the literature.[34] We have chosen here to represent the PEG density of the conjugates based on NMR results, following previous literature.[34,35]

Light scattering was used to ascertain the size and surface charge of the conjugates. The results are also included in Table 1. With the increase in PEG1000 surface density, a gradual increase in hydrodynamic diameter from 3.6 nm (0 PEG) to ca. 8 nm (25 PEG) was observed. While a direct comparison cannot be made, owing to a lack of literature pertaining the DLS analysis of $G3NH_2$-nPEG1000, several studies have been published reporting a similar increase in size of dendrimers upon grafting their end groups with PEG of varying MWs.[33,37,38] More detailed discussion and comparison with the literature is provided in the Supporting Information. A gradual decrease in the surface charge of the conjugates from +15.5 mV ($G3NH_2$-0PEG1000) to −4.7 mV ($G3NH_2$-25PEG1000) was observed upon increase in PEG density. Shielding of the positive charges in the dendrimers was actually observed even at the lowest PEG density, as the addition of 5PEG1000 decreased the surface charge to +1.1 mV. This drastic shift and decrease in surface charge has also been reported in several previous studies where PEG has been tethered to PAMAM dendrimer surface.[33,37,38,39]

The fact that PEGylation has such a dramatic impact on the size and surface charge of the dendrimers is of relevance, as those characteristics of the nanocarriers are expected to also impact the rate, extent, and mechanism of cellular uptake,[23,36,40−42] and their transport across epithelial barriers thereby aiding in modulation of their transport across the pulmonary epithelium. It has been shown that PEGylated dendrimers can interact and subsequently open tight junctions of Caco-2 cells even at low PEG surface density and relatively low concentrations.[37] In general, it has been shown that hydrophilic compounds are predominantly transported paracellularly through epithelial barriers[37,43,44] and that this process is cell dependent.[37,41,45,46] In the sections that follow we will demonstrate that the rate and extent of $G3NH_2$ nanocarrier internalization into and transport across models of the pulmonary epithelium can be modulated upon PEGylation.

**4.2. Cytotoxicity of $G3NH_2$-nPEG1000 on Calu-3 Cells.** Cytotoxicity of $G3NH_2$-nPEG1000 was evaluated on Calu-3 cells as described above. A summary of the cell viability results as a function of molar concentration of $G3NH_2$-nPEG1000 is shown in Figure 1.

As a general trend, $G3NH_2$-nPEG1000 had no appreciable inhibitory potential at concentrations below 0.01 μmol, with cell viabilities largely maintained at above 80%. While a 30% cell kill was observed for $G3NH_2$-0PEG1000 at a concentration of 1 μmol, over 90% of cells exposed to the PEGylated conjugates were viable at the same concentration. Further increase in concentration resulted in a reduction in cell viability for all conjugates, except for $G3NH_2$-25PEG1000. The minimum inhibitory concentration required to kill 50% of viable cells ($IC_{50}$) for $G3NH_2$-0PEG1000 was estimated to be 55 μmol. However, for concentrations below 100 μmol, none of the PEG terminated conjugates had exerted a 50% cell kill at 24 h incubation. On the basis of the observed trend, the $IC_{50}$ for $G3NH_2$-5PEG1000 and $G3NH_2$-13PEG1000 can be estimated to be greater than 100 μmol. Cells incubated in $G3NH_2$-25 PEG1000 had viability greater than 85% even at 100 μmol.

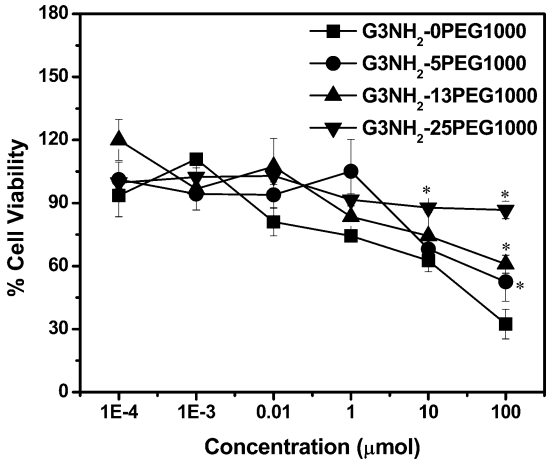


**Figure 1.** Viability of Calu-3 cells by MTT assay after incubation in $G3NH_2$-nPEG1000 conjugate laden media for 24 h. Cells incubated in serum-free culture medium (DMEM) were used as control. Results denote mean ± SD ($n$ = 5). * denotes statistically significant data ($p$ < 0.05) with respect to (w.r.t.) control ($G3NH_2$-0PEG1000).

While no prior work on the effect of dendrimers on viability of Calu-3 cells has been reported, comparing and contrasting the results from this work with those published on other relevant epithelial cell culture models like Caco-2 indicate that the PEGylated dendrimers have little to no cytotoxic effect reaffirming the improved toxicity profile of PEGylated dendrimers.[16,34,38,47,48] The benign nature imparted by PEGylation of cationic dendrimers has also been documented for other cell lines.[16,18,49]

**4.3. Culture of Calu-3 Cells, SEM, and Immunocytochemical (IC) Analysis.** The human airway epithelial cell line Calu-3 was used as an *in vitro* model to determine the effect of PEGylation on the permeability and uptake of $G3NH_2$-nPEG1000. Calu-3 is a well-differentiated and well-characterized cell line derived from human bronchial submucosal glands.[50] Besides forming tight junctions, Calu-3 cells have also been documented to possess many salient characteristics of the bronchial epithelium, viz. airway surface liquid, cilia, and the production of mucins and other immunologically active substances that make this cell line an appropriate candidate for elucidating tracheobronchial permeability and uptake *in vitro*.[50,51] In order to ensure that the cell monolayers are of requisite morphology for the transport studies, they were characterized via electrophysiological measurements (TEER), SEM, and immunocytochemistry.

AIC was adopted as Calu-3 cultured under those conditions is known to exhibit all salient features of native epithelium upon proliferation.[19,52] The cultures became confluent 6 days after culture under AIC. Monolayer confluence was evaluated by periodically recording TEER. A plot of the epithelial resistance achieved by the cell monolayer as a function of time (days in culture) is shown in Figure 2a. Under AIC, the TEER values of the cultured Calu-3 monolayer increased above the baseline values after about 5 days in culture and peaked by day 11 at ca. 305 Ω·cm$^2$. TEER values between ca. 300 and 350 Ω·cm$^2$ are considered to be an indicator of attainment of monolayer confluence and formation of tight junctions.[19,51,52]

Prior to beginning the transport experiments, once the TEER values peaked, immunocytochemical (IC) analysis and electron microscopy studies were conducted to visually ascertain the presence of tight junctions and morphology of the polarized


DOI: 10.1021/mp500662z
*Mol. Pharmaceutics* 2015, 12, 826−838

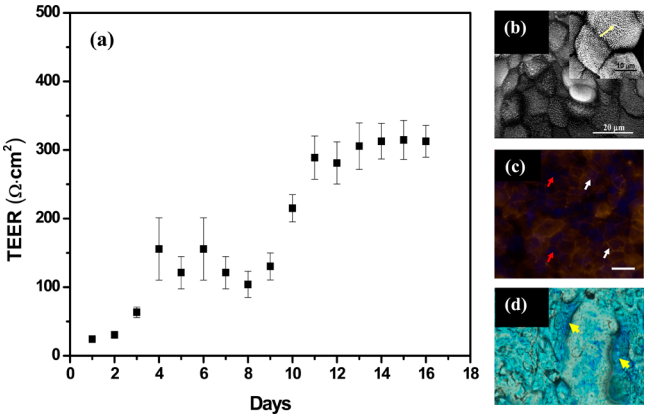


**Figure 2.** (a) Increase in transepithelial electrical resistance (TEER) of Calu-3 cells cultured under AIC on 0.33 $cm^2$ Transwell inserts as a function of time. Data represents mean ± SD ($n$ = 16). (b) SEM micrographs showing the morphology of AIC cultured Calu-3 cell monolayers, imaged once, where TEER values peaked and stabilized (day 15). Bar represents 20 $\mu$m. (Inset) A magnified SEM image of Calu-3 cell monolayer indicating the presence of microvilli and cilia (yellow arrow). Bar represents 5 $\mu$m. (c) Representative XY-2D sections of confluent Calu-3 monolayers captured using a confocal microscope at 40× magnification. Monolayers were fixed with 2% paraformaldehyde and stained for ZO-1 (white arrows), a tight junctional protein. Cell monolayers were also counterstained with DAPI (blue; red arrows) to show the location of the nucleus. Size bar indicates 20 $\mu$m. (d) Optical micrograph of a Calu-3 monolayer stained with the mucosal stain, Alcian blue indicating the presence of glycoproteins on the cell surface (yellow arrows).

Calu-3 monolayers. The cell monolayers were prepared for both studies as detailed in the methods section. Figure 2b is a representative electron micrograph of a Calu-3 monolayer fixed and stained and represents the nature of the monolayer at the time transport experiments commenced. In the same figure, as an inset, a higher magnification image of the monolayer is also shown. The presence of microvilli populating the surface of Calu-3 cells can be clearly observed from the electron micrograph. A closer inspection of the inset in Figure 2b reveals the presence of cilia (filled yellow arrow). Furthermore, we also observed the presence of mucus on the cell surface through electron microscopy (image not shown), another confirmation that the cell monolayer cultured under AIC possessed the requisite morphology mimicking the tracheobronchial epithelium.

IC analyses were also performed on selected confluent Calu-3 monolayers prior to commencing transport experiments. Studies were conducted to detect the presence of ZO-1 proteins, which are expressed in the tight junctions of polarized Calu-3 cells.[50,51] The presence of the protein was detected by staining the fixed cells with an anti-ZO-1 antibody labeled with a fluorescent dye, Alexa Fluor 546. The cells were counterstained with the nuclear stain, DAPI. Representative images (fluorescent microscope) of the fixed and stained Calu-3 cells monolayer is given in Figure 2c. The clear orange patterns observed along the periphery of the individual cells of the monolayer can be attributed to the presence of ZO-1, denoted by the white arrows. The presence of dark blue (red arrows) within the cell milieu indicates the nuclei of the cells. Alcian Blue stain was utilized to detect the presence of glycoproteins on the surface of the Calu-3 monolayer. An optical image of a monolayer stained with Alcian Blue is shown in Figure 2d. The distinct blue layer blanketing the cell surface (indicated by yellow arrows) can be attributed to the presence of mucosal glycoproteins. Furthermore, the confluence of Calu-3 was further established by measuring the apparent permeability ($P_{app}$) of a commonly used paracellular marker, sodium fluorescein (NaF). $P_{app}$ (A→ B) from this study was determined to be 2.8 ± 0.5 × $10^{-7}$ cm·$s^{-1}$, which is within the range of values reported in the literature, affirming the confluence of the monolayer.[19,53] Through a combination of TEER, IC, and SEM and transport of NaF, it can be concluded that the monolayers are confluent and have appropriate morphology, and monolayers grown at those conditions can thus be utilized for transport experiments, which are detailed in the section that follows.

**4.4. *In Vitro* Transport of G3$NH_2$-nPEG1000 Across Polarized Calu-3 Monolayers.** In this section we discuss the effect of PEGylation on the transport of G3$NH_2$-nPEG1000 conjugates across confluent Calu-3 monolayers cultured under AIC. The results are summarized in Figures 3 and 4. Figure 3

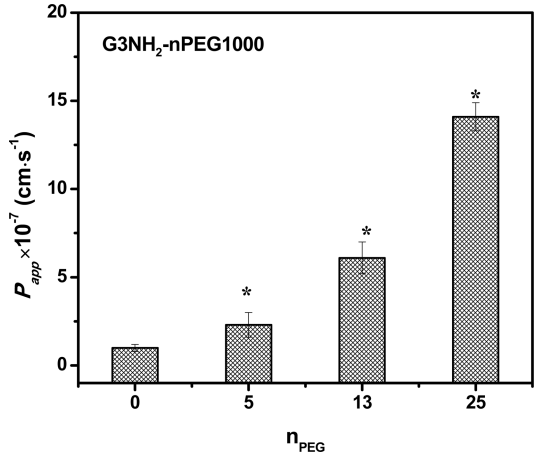


**Figure 3.** Effect of PEGylation density ($n_{PEG}$) on the apparent permeability ($P_{app}$) of G3$NH_2$-nPEG1000 conjugates across confluent Calu-3 monolayers. Reported $P_{app}$ values determined at the 5 h time point after incubation of the cell monolayers with conjugates. Data represents mean ± SD ($n$ = 4). Twenty-five nanomoles of conjugates in 1× HBSS was pulsed on the apical side. * denotes statistically significant data ($p$ < 0.05) with respect to control ($n_{PEG}$ = 0).

depicts the effect of PEG density on the $P_{app}$ of the nanocarriers. $P_{app}$ is a parameter that represents the ease with which compounds are transported across epithelial barriers.[19] The amount of dendrimer transported across the monolayer was assessed by determining the fluorescence emanating from FITC conjugated to the PEGylated dendrimers. The fluorescence in the receiving compartment was compared against previously constructed calibration curves prepared using FITC-labeled dendrimer constructs. The stability of FITC and PEG to PAMAM dendrimers at 37 °C and physiological pH has been well documented in several previous publications.[54−57]

Our results indicate that the $P_{app}$ of the G3$NH_2$-nPEG1000 nanocarriers across Calu-3 monolayers increases with increasing PEG1000 density. The $P_{app}$ for G3$NH_2$-0PEG1000 was determined to be 1.2 × $10^{-7}$ cm·$s^{-1}$, while that for G3$NH_2$-25PEG1000 was over 10-fold greater, at 14 × $10^{-7}$ cm·$s^{-1}$. The $P_{app}$ values for the all conjugates containing PEG1000 moieties were determined to be statistically significant ($p$ < 0.05)


DOI: 10.1021/mp500662z
Mol. Pharmaceutics 2015, 12, 826−838

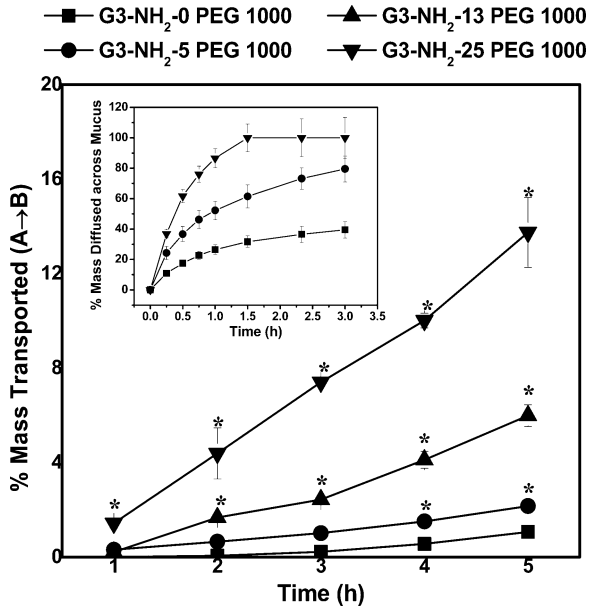


**Figure 4.** Effect of PEGylation density ($n_{PEG}$) on the cumulative mass of the G3NH$_2$-nPEG1000 conjugate transport across confluent Calu-3 monolayers (apical → basolateral) as a function of time. Error bars denote SD ($n$ = 4). Error bars not shown are smaller than symbol size. Twenty-five nanomoles of conjugates in 1× HBSS was pulsed on the apical side. * denotes statistically significant data ($p$ < 0.05) with respect to control ($n_{PEG}$ = 0). (Inset) Effect of PEGylation on the diffusion of G3NH$_2$-nPEG1000 conjugates across regular synthetic mucus.

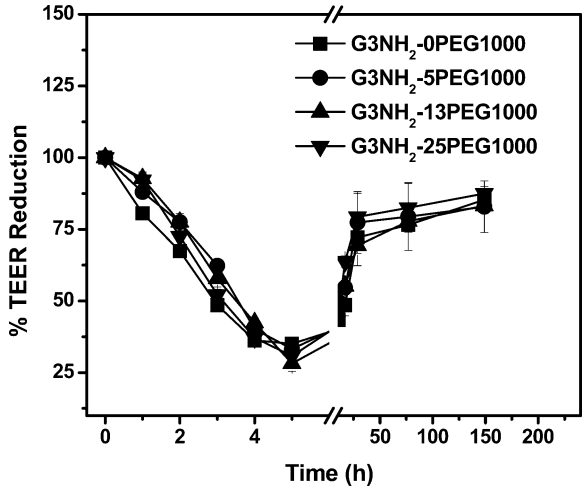


**Figure 5.** Effect of PEGylation density ($n_{PEG}$) of the G3NH$_2$-nPEG1000 conjugates (in 1× HBSS (pH 7.4)) on the TEER values of AIC cultured Calu-3 cells as a function of time. Values shown in the plot are denoted as % of control, which is TEER of Calu-3 incubated in 1× HBSS before the start of transport experiments. The recovery of TEER after the transport experiments is also shown in the plot. The cell monolayers were washed after the transport studies and reincubated in DMEM, and the TEER was monitored with time.

compared to the $P_{app}$ of the conjugate with no PEG (G3NH$_2$-0PEG1000).

In Figure 4, the cumulative mass of the conjugate transported from the apical to the basolateral side (A → B) of the inset is shown as a function of time. At 5 h, only ca. 1% of the G3NH$_2$-0PEG1000 had been transported to the basolateral side. With conjugation of PEG1000 to the G3NH$_2$ surface, an increase in the rate of mass of conjugate transported was observed, with as much as 12% for G3NH$_2$-25PEG1000. All the PEGylated conjugates, viz., G3NH$_2$-5PEG1000, G3NH$_2$-13PEG1000, and G3NH$_2$-25PEG1000, had statistically significant increases in the mass transported ($p$ < 0.05) compared to that seen for G3NH$_2$-0PEG1000, at all times, as shown in Figure 4.

As an inset to Figure 4, we show the effect of PEGylation on the diffusion of G3NH$_2$-nPEG1000 conjugates across regular synthetic mucus. It illustrates the fact that the more PEGylated nanocarriers (greater PEG surface density) are capable of diffusing much faster through the mucus layer compared to less PEGylated carrier. The initial rate of transport ($R_0$) was determined to be 3.0, 5.8, and 9.8 $\mu g \cdot h^{-1}$ for the dendrimers with 0, 5, and 25PEG1000, respectively, and G3NH$_2$-13PEG1000. It suggests that the charge of the carrier seems to greatly affect its transport even at sizes much smaller than the mucus mesh size.[14,58]

In order to evaluate the effect of the PEGylation of the conjugates on the tight junctions, changes in electrophysiological behavior were monitored by recording the TEER during the course of the transport experiments. The results are summarized in Figure 5.

From Figure 5, it is evident that G3NH$_2$-nPEG1000 had a pronounced effect on the tight junctional properties of the monolayer. A gradual reduction in the TEER of Calu-3 monolayers was observed during the course of the transport experiments, with all conjugates reducing the TEER of the monolayers to ca. 30% of the original value of cells incubated in HBSS only. This phenomenon was largely reversible, as upon reincubating the monolayers with culture media in the absence of the conjugates, the TEER values returned to ca. 80% of their original value within 3 days of incubation, as seen in Figure 5. A similar reduction in TEER has been reported in the case of Caco-2 cells, upon incubation with PEG-surface modified G3NH$_2$ and G4NH$_2$.[59] The presence of conjugates resulted in a decrease in TEER down to 20% of the original value, and reincubation in dendrimer-free medium restored the TEER back to original levels.

Transport of surface-modified dendrimers across epithelial monolayers is highly dependent on the size, surface charge, the chemistry of functionalities attached to the surface, and the cell type.[18,37,60] Previous studies have suggested that dendrimers transport across monolayers via a combination of transcellular (through the cell milieu) and paracellular (through the tight junctions) routes.[18,37] Most transport studies of PAMAM have focused on cell lines in the context of oral delivery, however, with Caco-2, IPEC-J2, and Madin-Darby Kidney cells being the primary *in vitro* models.[18,45] To the best of our knowledge, the permeability characteristics of PEGylated G3NH$_2$ conjugates (or any dendrimer) have not been evaluated on cell culture models relevant to the pulmonary epithelium.

Conjugation of a lipid, lauroyl chloride, to G3NH$_2$ surface increased $P_{app}$ across Caco-2 monolayers by a factor of 2.5 from ca. $2 \times 10^{-6}$ cm·s$^{-1}$ to ca. $5 \times 10^{-6}$ cm·s$^{-1}$ within a 3 h time period, possibly due to the permeation enhancing effects of the lipid chains.[36] In another study, addition of polyamines (ornithine and arginine) onto the G4NH$_2$ surface also improved the permeability of the conjugates across Caco-2 and IPEC-J2 cell monolayers after 3 h, possibly due to a combination of polyamine transporter system aiding in the active uptake of the conjugates and a passive transport through the tight junctions due to charge mediation.[60,61]


DOI: 10.1021/mp500662z
*Mol. Pharmaceutics* 2015, 12, 826−838

In this work we observed that as the surface density of PEG increases, the transport of $G3NH_2$-nPEG1000 across the Calu-3 polarized monolayer also increased. Because all $G3NH_2$-nPEG1000 impact the tight junctions to the same extent, at least as probed by the ionic mobility across the epithelial barrier (TEER), we argue that this enhanced transport for $G3NH_2$-nPEG1000 with higher number of graft PEGs, compared to those with lower PEG density does not reflect a permeation enhancement effect. The fact that all $G3NH_2$-nPEG1000, irrespective of size and surface charge, affect the TEER to the same degree is, to some extent, surprising, as tight junctional proteins are negatively charged and have gaps on the order of 0.8−2 nm depending on cell type.[62] One would have expected, therefore, that the smaller and more positively charged dendrimers would have exerted a greater influence on TEER. Interestingly, it has been shown that tethering of 1 or 2 chains of PEG (MW 750 Da) onto G3.5 and G4.5 dendrimers (hydroxyl terminated dendrimers) decreased the transepithelial permeability of the conjugates across Caco-2 monolayers after 2 h of incubation, possibly due to relatively lower levels of interaction of PEG modified conjugates with the tight junctions of Caco-2.[37] However, the trend observed here indeed seems to be somewhat universal for positively charged polymers, as PEG modified chitosan, a linear polymer with $-NH_2$ groups (MW PEG 1900 Da), also reduces the TEER of Calu-3 - down to 40% of the initial value.[63] It was suggested that the reduction in the TEER could be due to the higher equivalent concentrations of chitosan in the conjugates in combination with the unsubstituted amine groups of the PEG modified chitosan backbone.[63] It should be noted, however, that TEER is a surrogate for the direct measurement of transport, and care should be taken when analyzing these measurements.

Another interesting observation was the rapid increase in the transport of $G3NH_2$-25PEG1000 within the first hour when compared to the other conjugates (ca. 1.4% compared to 0.3% in the case of $G3NH_2$-5PEG1000). The presence of PEG on nanocarrier surfaces (in that particular case of solid nanoparticles, hundreds of nanometers) has been shown to impart stealth-like properties to them thereby facilitating their rapid transport across mucosal barriers.[64,65] Combining the results discussed above, with the fact that internalization of the carriers within Calu-3 cells decreases upon PEGylation (discussed below), one could argue that a fast transport across the mucosal layer and decreased interaction with and internalization within Calu-3 cells may provide an opportunity for the more densely PEGylated nanocarriers to achieve enhanced transport across the monolayer. Of course this assumes a dominant paracellular transport, which seems plausible given the results at hand, but has not been definitely established in this work. These studies are ongoing in our laboratories.

**4.5. Cellular Uptake.** The effect of PEGylation on the extent of cellular uptake of the $G3NH_2$-nPEG1000 conjugates into polarized Calu-3 monolayers was determined. Cellular internalization was evaluated by cell lysate and flow cytometry. The cell lysate results at the end point of transport studies (5 h) are plotted as % uptake in Figure 6.

At the end of the transport studies (5 h time point), ca. 10% of the $G3NH_2$-0PEG1000 was internalized into Calu-3 cells. In contrast, PEGylated conjugates had reduced internalization. The total internalized amount (mass basis relative to the amount of dendrimer added in the beginning of the transport study) for $G3NH_2$-5PEG1000, $G3NH_2$-13PEG1000, and $G3NH_2$-25PEG1000 was 6%, 2.2%, and 1.7%, respectively.

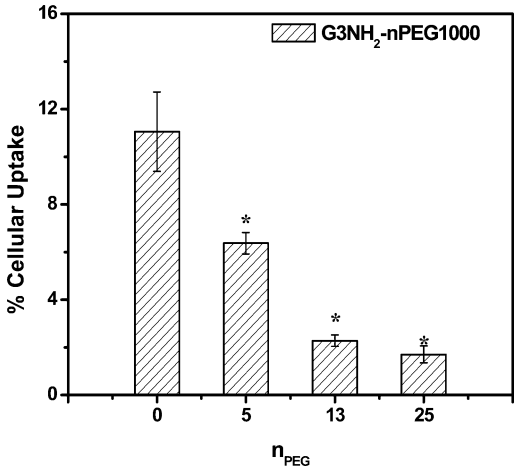


**Figure 6.** Effect of PEGylation density ($n_{PEG}$) of the $G3NH_2$-nPEG1000 conjugates on the % uptake into Calu-3 at $t$ = 5 h, as measured in the cell lysates. Values represent mean ± SD ($n$ = 4). * denotes statistically significant difference ($p < 0.05$) with respect to control ($n_{PEG}$ = 0).

These results, combined with the determination of the amount of dendrimer left in the apical side of the insert at the end of the transport studies, and the cumulative amount collected on the basolateral side also at 5 h, allowed us to perform an overall mass balance study. The results yielded a total average recovery of ca. 80% for all conjugates. The ca. 20% not recovered could be attributed to factors including the presence of conjugates bound to cell surface that remain adhered to cell debris after lysis and the adsorption of conjugates to surfaces of the inserts and wells.

In addition to determining cellular uptake through cell lysis, internalization of the conjugates was monitored as a function of time using flow cytometry. The results of the study are summarized in Figure 7a. The studies were conducted on polarized Calu-3 monolayers as detailed before. Proliferation of Calu-3 until polarization is essential as it facilitates the formation of tight junctions thereby providing a more accurate representation of the true airway morphology.[66] Figure 7a is a plot of the mean fluorescence intensity (MFI) as a function of time.

From the plot, it is observed that the cellular uptake is reduced as the PEG number on the $G3NH_2$ surface increases, in agreement with what was observed from the cell lysate experiments. However, here we also obtain the kinetics of the process. The maximum cellular uptake was observed for $G3NH_2$-0PEG1000, whose uptake saturates by the 5 h time point, as evidenced by the leveling off of the MFI values. This trend in cellular internalization for $G3NH_2$-0PEG1000 can be attributed to the typical trafficking mechanism of cationic dendrimers, which are believed to be taken up by charge mediated endocytosis, facilitated by the presence of negatively charged proteoglycans on cell surface.[23] However, the rates of internalization were gradually reduced with the increase in PEG density, in spite of their faster extracellular transport, again in agreement with the cell lysate studies. The $R_o$ for $G3NH_2$-25PEG1000 was 27.5 FIU·$h^{-1}$ (FIU = fluorescence intensity units), while $R_o$ for $G3NH_2$-0PEG1000 was calculated to be 73.5 FIU·$h^{-1}$.

Additionally, it is interesting to note that the saturation in uptake observed in the case of the non-PEGylated dendrimer was not seen for the PEGylated carriers, suggesting that


DOI: 10.1021/mp500662z
Mol. Pharmaceutics 2015, 12, 826−838

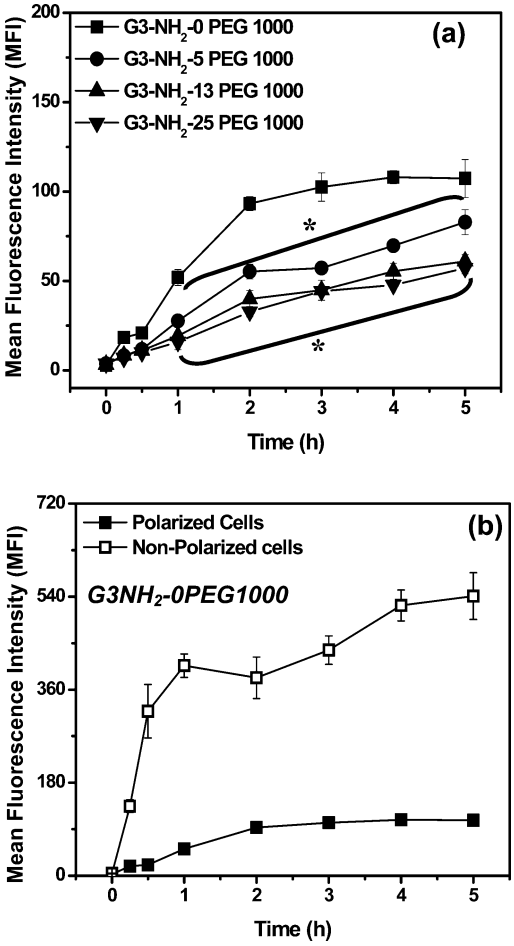


**Figure 7.** (a) Effect of PEGylation density ($n_{PEG}$) on the cellular uptake of the $G3NH_2$-nPEG1000 conjugates into polarized Calu-3 cell monolayers as a function of time, as determined by flow cytometry. Data represents mean ± SD ($n = 6$). * denotes statistically significant difference ($p < 0.05$) with respect to control ($G3NH_2$-0PEG1000). (b) Effect of polarization of the Calu-3 monolayers on the uptake of $G3NH_2$-0PEG1000.

PEGylation may also cause a modulation in the route of internalization into Calu-3 cells. It is also possible that saturation will be reached at later times than compared to the non-PEGylated system, but the faster transport of the PEGylated nanocarriers through mucus and thus presentation to the cell surface (inset Figure 4) seems to suggest that this is not the case. Surface functionalities of dendrimers have been shown to affect not only the rate and amount of internalization but also the endocytic mechanism upon which internalization takes place.[18,23,37,67] PEGylation of the conjugates results in the shielding of charges, which minimizes the interaction of the conjugates with the cell surface, resulting in reduced surface adsorption that would subsequently lead to endocytosis.[37] For instance, in an earlier study involving partial PEGylation of $G4NH_2$ conjugates, an increase in surface coverage of PEG 5000 Da resulted in a significant decrease in the cellular uptake in B16F3 cells, as quantified by flow cytometry. Furthermore, it was observed that this reduction had a definite correlation to the zeta potential of the conjugates, thus reiterating the potential impact of surface charge and surface functionality on cellular uptake.[38] Previous works have also shown that conjugation of PEG 750 Da to the surface of G3.5 PAMAM dendrimers reduced interaction with the Caco-2 cell surface. Interestingly, the same study reported that addition of the same PEG moiety to G4.5 dendrimers increased cellular uptake, suggesting that an ideal charge density may be required for promotion or reduction of dendrimer trafficking into the cellular milieu.[37]

Uptake experiments reported here were conducted on polarized, well differentiated monolayers of Calu-3. Polarized Calu-3 monolayers form tight junctions and exhibit morphological features native to the pulmonary epithelium.[50] The importance of cell polarization in the cellular uptake of the $G3NH_2$ in Calu-3 cells was evaluated, and the results shown in Figure 7b, where the uptake results in polarized cells are contrasted with nonpolarized monolayers. Nonpolarized Calu-3 monolayers were able to internalize $G3NH_2$-0PEG1000 to a much greater extent compared to the polarized cells as evidenced by a 5-fold increase in the MFI values for the nonpolarized cells. Another interesting observation to note from this figure is the lack of saturation in the uptake of the conjugate exposed to the nonpolarized cells when compared to the polarized Calu-3 monolayers. The effect of Calu-3 polarization was also observed in other independent studies where it was reported that well-formed, polarized airway epithelial cells were infected to a lesser extent with *Pseudomonas aeruginosa* and *Chlamydia trachomatis* compared to their nonpolarized counterparts.[66,68] These results combined suggest that it is essential to conduct cellular uptake studies of moieties on polarized, well characterized cell monolayers in order to understand the true extent and kinetics of internalization on airway epithelial models as was done in the studies described here.

Through the collective set of experiments comprising *in vitro* transport and cellular uptake assessed by cell lysis and flow cytometry, transport, and TEER, we can gauge the impact of PEGylation on the transport and uptake of $G3NH_2$-nPEG1000 across and into Calu-3 monolayers. The results showcased through these studies suggest that by suitably tailoring the surface of $G3NH_2$ with PEG1000 one can achieve a great deal of modulation in both transport and cellular uptake of DNCs across and into such a relevant model of the pulmonary epithelium. The results obtained here also suggest that conjugation of PEG can impart other beneficial characteristics to the $G3NH_2$ nanocarriers, by reducing their toxicity and assisting in overcoming extracellular barriers present in the pulmonary epithelium, such as the mucosal layer.

These results can be utilized to guide the design of polymeric nanocarriers for controlled and targeted local or systemic delivery of therapeutics to (regional delivery) and through (systemic circulation) the lungs. Carriers with reduced transport and enhanced cellular internalization are potential candidates for the regional targeting of drugs to the lungs, while those that rapidly transport across the pulmonary epithelium are potential candidates to target the systemic circulation.

While in the previous sections we evaluated the feasibility of using PEGylation to modulate the transport of $G3NH_2$ nanocarriers across the pulmonary epithelium using an *in vitro* model, in the section that follows we evaluate the effect of PEGylation on the transport of $G3NH_2$-nPEG1000 across an *in vivo* model of the lung epithelium, by determining the pharmacokinetic (PK) behavior of selected nanocarriers upon inhalation administration to Balb/c mice.

**4.6. *In Vivo* Pharmacokinetic (PK) Evaluation of $G3NH_2$-nPEG1000.** The plasma concentration−time profiles for the $G3NH_2$-nPEG1000 dendrimer conjugates following


DOI: 10.1021/mp500662z
*Mol. Pharmaceutics* 2015, 12, 826−838

pharyngeal aspiration (PA) are shown in Figure 8a. The results for i.v. administration are shown in Figure 8b.

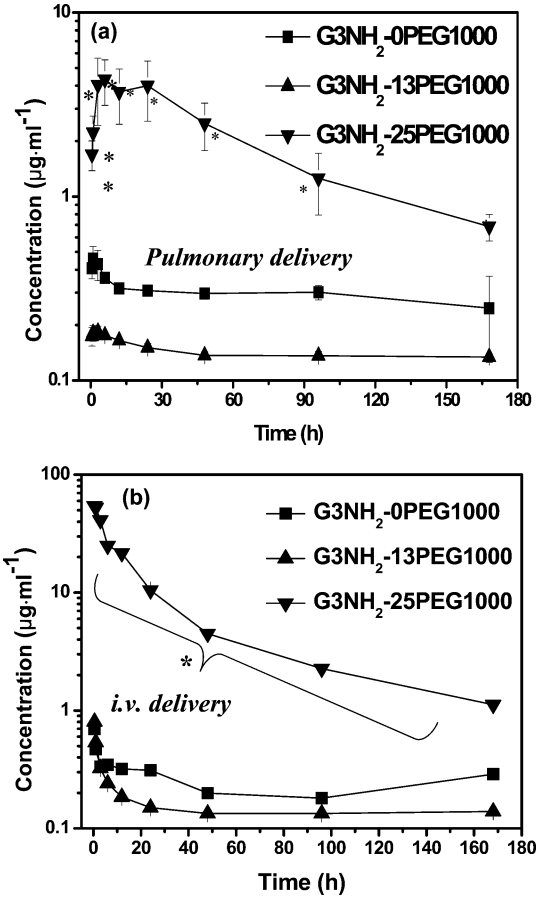


**Figure 8.** Mean plasma concentrations of $G3NH_2$-nPEG1000 conjugates detected by fluorometry after (a) pulmonary administration (PA) in mice ($n$ = 6 for each condition) as a function of time, and (b) after intravenous (i.v.) administration in mice ($n$ = 3). In both cases, blood samples were collected from the tail vein using the tail bleeding method. Statistical significance with respect to control for panel a ($p$ < 0.05) is denoted by *.

The PK parameters calculated from plasma concentration versus time profiles (Figure 8) are shown in Table 2:

The results show that the dendrimers with the highest degree of PEGylation ($G3NH_2$-25PEG1000) have the highest plasma concentrations at all time points. After PA of the $G3NH_2$-25PEG1000 conjugate, a peak plasma concentration of 4.6 $\mu$g was reached at 5 h and stayed constant for ca. 24 h. The plasma concentration then slowly decreased, with dendrimer remaining in plasma even at the end of 1 week. In contrast, $G3NH_2$-0PEG1000 and $G3NH_2$-13PEG1000 had significantly lower peak plasma concentrations at 0.5 and 0.2 $\mu$g, respectively. It is important to note, however, that, while the values for the $G3NH_2$-0PEG1000 and $G3NH_2$-13PEG1000 were low, they were well above the background detection limit for the PK assay.

Among the conjugates, $G3NH_2$-25PEG1000 had the highest plasma concentration at the first time point tested following i.v. administration (30 min). The $G3NH_2$-0PEG1000 and $G3NH_2$-13PEG1000 dendrimers already had significant plasma clearance by the first time point. This rapid clearance prior to our initial time point indicates a limitation of our data with missed kinetics 0−30 min. This limits the use of absolute pharmacokinetic calculations; particularly bioavailability, which would be dependent on an accurate AUC for 0−30 min following i.v. administration. However, relative pharmacokinetics (i.e., exposure) of the conjugates can still provide meaningful comparative analysis. The total plasma clearance calculated from the i.v. administered mice was the highest for $G3NH_2$-13PEG1000 at 11.67 mL·min$^{-1}$, while the lowest clearance was observed for $G3NH_2$-25PEG1000 (0.12 mL·min$^{-1}$). An increase in PEG surface density, therefore, reduces clearance (as evidenced by a lower clearance and elimination rate constant, $K_{el}$) and increases circulation time (as evidenced by the much higher half-life, $T_{1/2}$). This is likely due to the glomerular size cutoff of 10 nm enabling quick renal clearance of $G3NH_2$-0PEG1000 and $G3NH_2$-13PEG1000, but not of the $G3NH_2$-25PEG1000.[69] It is also well established that PEGylation increases the circulation time of various nanocarriers in the systemic circulation by way of increasing the hydrophilicity of the carrier and reducing opsonization, drastically reducing uptake by the mononuclear phagocytic system (MPS).[16,22]

Following pulmonary administration of $G3NH_2$-25PEG1000 both the $C_{max}$ and $T_{max}$ are significantly higher than the other formulations, resulting in a very high plasma exposure (high AUC). Given the reduced clearance of the $G3NH_2$-25PEG1000 dendrimer from i.v. studies, a relatively high AUC was to be expected. However, on the basis of the *in vitro* studies that show much greater transport through the pulmonary epithelium, one could expect that a faster rate of absorption could also be a contributing mechanism toward determining the high AUC of $G3NH_2$-25PEG1000. To test this hypothesis, the absorption rate constant ($K_a$) of $G3NH_2$-25PEG1000 from the lungs was calculated. The $K_a$ determined for $G3NH_2$-25PEG1000 is 0.85

**Table 2. Pharmacokinetic Parameters for the $G3NH_2$-nPEG1000 upon Pulmonary (Pharyngeal Aspiration: PA) and i.v. Administration to Mice; Results Represent Mean ± SD ($n$ = 6)**

| PK properties | $G3NH_2$-0PEG1000 | $G3NH_2$-13PEG1000 | $G3NH_2$-25PEG1000 |
|---|---|---|---|
| $Cl$ (mL/min)[a] | 11.67 ± 3.94 | 17.67 ± 2.11 | 0.12 ± 0.08 |
| $K_{el}$ (h$^{-1}$)[a] | 0.025 ± 0.01 | 0.027 ± 0.01 | 0.013 ± 0.0001 |
| $T_{1/2}$ (h)[a] | 29.62 ± 9.51 | 25.86 ± 4.78 | 53.01 ± 0.34 |
| $AUC_{iv}$ (ng·h/ml)[a] | 4540 ± 670 | 5840 ± 440 | 1194980 ± 38310 |
| $T_{max}$ (h)[b] | 1.33 ± 0.82 | 2.5 ± 1.97 | 5 ± 1.55 |
| $C_{max}$ (ng/mL)[b] | 460 ± 60 | 190 ± 10 | 4600 ± 144 |
| $K_a$ (h$^{-1}$)[b] | 0.40 ± 0.22 | 0.14 ± 0.07 | 0.85 ± 0.15 |
| $AUC_{PA}$ (ng·h/ml)[b] | 4460 ± 290 | 4000 ± 140 | 376640 ± 96950 |

[a]Data derived from i.v. experiments. [b]Data derived from PA experiments.



DOI: 10.1021/mp500662z
*Mol. Pharmaceutics* 2015, 12, 826−838

$\pm$ 0.15 $h^{-1}$ and is indeed much greater than that determined for $G3NH_2$-0PEG1000 and $G3NH_2$-13PEG1000 of 0.4 $\pm$ 0.22 $h^{-1}$ and 0.14 $\pm$ 0.07 $h^{-1}$, respectively. Combined, these results suggest that both a reduced clearance and increased absorption contribute to the high AUC of $G3NH_2$-25PEG1000, which is corroborated by the high *in vitro* transport rates for that dendrimer.

It is also interesting to contrast our results with a recent publication of the effect of size/molecular weight on pulmonary absorption of PEGylated polylysine (PLL) dendrimers.[70] That study shows that, at the lower molecular weight range of PLL dendrimers (between 11 and 22 kDa), the systemic absorption from the lungs upon intratracheal administration did not change significantly, ranging between 17 and 31%, and was much higher than that of a PEGylated PLL with much higher MW (78 kDa), which showed a 2% absorption only. The MW range of the PEGylated PAMAM dendrimers in our work is close to the 11−22 K range and suggests that the effects in plasma exposure seen here are indeed a strong function of PEGylation density.

When considering PK of the dendrimer systems after both pulmonary and i.v. exposure, these results suggest that change in surface chemistry of the PAMAM dendrimers upon PEGylation has a significant effect on their pulmonary translocation. PEGylation up to a certain degree ($G3NH_2$-13PEG1000 in this case) reduces the rate of absorption of the dendrimers across the lungs, whereas a higher PEGylation ($G3NH_2$-25PEG1000) improves the absorption across the lungs in addition to increasing the circulation time and concentration of the dendrimers in the systemic circulation postabsorption from the lungs. The effect of PEGylation on the whole animal and lung tissue biodistribution of $G3NH_2$-nPEG1000 are under investigation in our laboratories and are expected to complement the results of this study.

## 5. CONCLUSIONS

In this work we determined the effect of PEGylation of DNCs on their interaction with *in vitro* and *in vivo* models of the pulmonary epithelium. The cellular uptake, transport, and pharmacokinetics of $G3NH_2$ dendrimers conjugated with PEG 1000 Da at various surface densities (5, 13, and 25 PEGs per $G3NH_2$ molecule) were studied. Cell viability studies conducted on Calu-3 cells revealed that PEGylation improved cell survival rate, with over 90% of cell viability at concentrations as high as 100 $\mu$mol when incubated with $G3NH_2$-25PEG1000 for 24 h. In contrast, only 30% of cells incubated with $G3NH_2$-0PEG1000 survived at the same concentration. *In vitro* transport studies conducted on polarized Calu-3 monolayers revealed an increase in transport of $G3NH_2$-nPEG1000 with increasing PEG density. As much as 14% (w/w) of $G3NH_2$-25PEG1000 are transported from the apical to the basolateral side of the monolayer at 5 h. However, only 1% of $G3NH_2$-0PEG1000 is transported within the same time. PEGylation also resulted in modulation of cellular uptake, as evidenced by flow cytometry and cell lysis studies, where PEGylation of DNCs was seen to decrease cellular uptake. Peak plasma concentrations of ca. 5 $\mu$g/mL was detected for $G3NH_2$-25PEG1000 by 3 h, while $G3NH_2$-0PEG1000 and $G3NH_2$-13PEG1000 had very low peak plasma values −0.2 and 0.4 $\mu$g/mL, respectively. The rate of absorption of the nanocarriers was also impacted upon PEGylation. The rate of absorption was seen to increase with PEGylation, albeit not in a linear fashion. These combined results suggest that surface modification of $G3NH_2$ with appropriate surface densities of PEG can aid in the modulation of transport and uptake of the nanocarriers into and across the pulmonary epithelium and thus can be potentially used to guide the design of such nanocarriers for treating either local (lung) diseases or targeting other tissues upon oral inhalation administration, using the lungs as an alternative noninvasive pathway to the bloodstream.

## ■ ASSOCIATED CONTENT

### Ⓢ Supporting Information

Descriptions of the synthesis and characterization of the various structures/conjugates, including NMR, MALDI, and FT-IR, along with a tabulation of molar ratios of the reactants for preparation of each dendrimer construct are provided. Cell culture and *in vitro* toxicity experiments are also provided. This material is available free of charge via the Internet at http://pubs.acs.org.

## ■ AUTHOR INFORMATION

### Corresponding Author

*Tel: +1-313-577-4669. Fax: +1-313-578-5820. E-mail: sdr@eng.wayne.edu.

### Notes

The authors declare no competing financial interest.

## ■ ACKNOWLEDGMENTS

B.B. and S.R.P.d.R. would like to acknowledge financial support from National Science Foundation (NSF-CBET grant no. 0933144) and the NanoIncubator at WSU. S.R.P.d.R. and B.B. would like to thank Profs. Verani's, Prof. Matthew's, and Prof. Huttemann's groups at Wayne State University, and Prof. Kannan's group, now at Johns Hopkins, for giving us access to their laboratory equipment, in particular, the FTIR, plate reader, fluorescence microscope, and DLS, respectively. The Microscopy, Imaging, and Cytometry Resources core is supported, in part by NIH center grant P30CA22453 to The Karmanos Cancer Institute, Wayne State University, and the Perinatology Research Branch of the National Institutes of Child Health and Development, Wayne State University. A.K.M. and J.R. would like to acknowledge financial support from the Department of Pharmaceutical Sciences and the NanoIncubator at WSU.

## ■ REFERENCES

(1) Cipolla, D. C.; Gonda, I. Formulation technology to repurpose drugs for inhalation delivery. *Drug Discovery Today* **2011**, *8*, 123−130.
(2) Patton, J. S.; Byron, P. R. Inhaling medicines: delivering drugs to the body through lungs. *Nat. Rev. Drug Discovery* **2007**, *6*, 67−74.
(3) Aurora, S. K.; Silberstein, S. D.; Kori, S. H.; Tepper, S. J.; Borland, S. W.; Wang, M.; Dodick, D. W. MAP0004, orally inhaled DHE: a randomized, controlled study in the acute treatment of migraine. *Headache* **2011**, *51* (4), 507−17.
(4) Dolovich, M. B.; Dhand, R. Aerosol drug delivery: developments in device design and clinical use. *Lancet* **2011**, *377* (9770), 1032−45.
(5) Merkel, O. M.; Kissel, T. Nonviral pulmonary delivery of siRNA. *Acc. Chem. Res.* **2011**, DOI: 10.1021/ar200110p.
(6) Agu, R. U. In vitro and in vivo testing methods for respiratory drug delivery. *Expert Opin. Drug Delivery* **2011**, *8* (1), 57−69.
(7) Azarmi, S.; Roa, W. H.; Lobenberg, R. Targeted delivery of nanoparticles for the treatment of lung diseases. *Adv. Drug Delivery Rev.* **2008**, *60*, 863−875.
(8) Inapagolla, R.; Guru, B. R.; Kurtoglu, Y. E.; Gao, X.; Lieh-Lai, M.; Bassett, D. J.; Kannan, R. M. In vivo efficacy of dendrimer-


DOI: 10.1021/mp500662z
*Mol. Pharmaceutics* 2015, 12, 826−838

methylprednisolone conjugate formulation for the treatment of lung inflammation. *Int. J. Pharm.* **2010**, *399* (1−2), 140−7.
(9) Menjoge, A. R.; Kannan, R. M.; Tomalia, D. A. Dendrimer-based drug and imaging conjugates: design considerations for nanomedical applications. *Drug Discovery Today* **2010**, *15* (5−6), 171−85.
(10) Misra, A.; Hickey, A. J.; Rossi, C.; Borchard, G.; Terada, H.; Makino, K.; Fourie, P. B.; Colombo, P. Inhaled drug therapy for treatment of tuberculosis. *Tuberculosis* **2011**, *91* (1), 71−81.
(11) Roy, I.; Vij, N. Nanodelivery in airway diseases: challenges and therapeutic applications. *Nanomed. Nanotechnol.* **2010**, *6* (2), 237−44.
(12) Rytting, E.; Nguyen, J.; Wang, X.; Kissel, T. Biodegradable polymeric nanocarriers for pulmonary drug delivery. *Expert Opin Drug Delivery* **2008**, *5*, 629−639.
(13) Davis, M. E.; Chen, Z.; Shin, D. M. Nanoparticle therapeutics: an emerging treatment modality for cancer. *Nat. Rev. Drug Discovery* **2008**, *7*, 771−782.
(14) Lai, S. K.; Wang, Y. Y.; Hanes, J. Mucus-penetrating nanoparticles for drug and gene delivery to mucosal tissues. *Adv. Drug Delivery Rev.* **2009**, *61* (2), 158−71.
(15) Pison, U.; Welte, T.; Giersig, M.; Groneberg, D. A. Nanomedicine for respiratory diseases. *Eur. J. Pharmacol.* **2006**, *533*, 341−350.
(16) Svenson, S. Dendrimers as versatile platform in drug delivery applications. *Eur. J. Pharm. Biopharm.* **2009**, *71* (3), 445−62.
(17) D'Emanuele, A.; Attwood, D. Dendrimer-drug interactions. *Adv. Drug Delivery Rev.* **2005**, *57* (15), 2147−62.
(18) Sadekar, S.; Ghandehari, H. Transepithelial transport and toxicity of PAMAM dendrimers: Implications for oral drug delivery. *Adv. Drug Delivery Rev.* **2011**, *64*, 571−588.
(19) Grainger, C. I.; Greenwell, L. L.; Lockley, D. J.; Martin, G. P.; Forbes, B. Culture of Calu-3 cells at the air interface provides a representative model of the airway epithelial barrier. *Pharm. Res.* **2006**, *23* (7), 1482−90.
(20) Zhang, X. Q.; Intra, J.; Salem, A. K. Conjugation of polyamidoamine dendrimers on biodegradable microparticles for nonviral gene delivery. *Bioconjugate Chem.* **2007**, *18* (6), 2068−76.
(21) Guillaudeu, S. J.; Fox, M. E.; Haidar, Y. M.; Dy, E. E.; Szoka, F. C.; Frechet, J. M. PEGylated dendrimers with core functionality for biological applications. *Bioconjugate Chem.* **2008**, *19* (2), 461−9.
(22) Jain, N. K.; Nahar, M. PEGylated Nanocarriers for Systemic Delivery. In *Cancer Nanotechnology: Methods in Molecular Biology*; Springer: New York, 2009; Vol. *624*, pp 221−234.
(23) Perumal, O. P.; Inapagolla, R.; Kannan, S.; Kannan, R. M. The effect of surface functionality on cellular trafficking of dendrimers. *Biomaterials* **2008**, *29* (24−25), 3469−76.
(24) Promega Corp. *CellTiter 96 $AQ_{ueous}$ Non-Radioactive Cell Proliferation Assay*; Promega: Madison, WI, 2009.
(25) Probes, M. *ZO-1, Mouse Monoclonal Antibody−Alexa Fluor 546*; Invitrogen: Grand Island, NY, 2010.
(26) Biotechnology, P. *Pierce BCA Protein Assay*; Thermo Scientific: Rockford, IL, 2011.
(27) Broughton-Head, V. J.; Smith, J. R.; Shur, J.; Shute, J. K. Actin limits enhancement of nanoparticle diffusion through cystic fibrosis sputum by mucolytics. *Pulm. Pharmacol. Ther.* **2007**, *20* (6), 708−717.
(28) Sanders, N.; Rudolph, C.; Braeckmans, K.; De Smedt, S. C.; Demeester, J. Extracellular barriers in respiratory gene therapy. *Adv. Drug Delivery Rev.* **2009**, *61* (2), 115−127.
(29) Bhat, P. G.; Flanagan, D. R.; Donovan, M. D. Drug diffusion through cystic fibrotic mucus: Steady-state permeation, rheologic properties, and glycoprotein morphology. *J. Pharm. Sci.* **1996**, *85* (6), 624−630.
(30) Sanders, N. N.; Van Rompaey, E.; De Smedt, S. C.; Demeester, J. Structural alterations of gene complexes by cystic fibrosis sputum. *Am. J. Respir. Crit. Care Med.* **2001**, *164* (3), 486−493.
(31) Sarlo, K.; Blackburn, K. L.; Clark, E. D.; Grothaus, J.; Chaney, J.; Neu, S.; Flood, J.; Abbott, D.; Bohne, C.; Casey, K.; Fryer, C.; Kuhn, M. Tissue distribution of 20 nm, 100 and 1000 nm fluorescent polystyrene latex nanospheres following acute systemic or acute and repeat airway exposure in the rat. *Toxicology* **2009**, *263* (2−3), 117−26.
(32) Gajbhiye, A.; Kumar, V. P.; Tekade, R. K.; Jain, N. K. Pharmaceutical and biomedical potential of PEGylated dendrimers. *Curr. Pharm. Des.* **2007**, *13*, 415−429.
(33) Kaminskas, L. M.; Boyd, B. J.; Karellas, P.; Krippner, G. Y.; Lessene, R.; Kelly, B.; Porter, C. J. The impact of molecular weight and PEG chain length on the systemic pharmacokinetics of PEGylated poly L-lysine dendrimers. *Mol. Pharmaceutics* **2008**, *5* (3), 449−63.
(34) Kim, Y.; Klutz, A. M.; Jacobson, K. A. Systematic investigation of polyamidoamine dendrimers surface-modified with poly(ethylene glycol) for drug delivery applications: synthesis, characterization, and evaluation of cytotoxicity. *Bioconjugate Chem.* **2008**, *19* (8), 1660−72.
(35) Kim, Y.; Hechler, B.; Klutz, A. M.; Gachet, C.; Jacobson, K. A. Toward multivalent signaling across G protein-coupled receptors from poly(amidoamine) dendrimers. *Bioconjugate Chem.* **2008**, *19* (2), 406−11.
(36) Jevprasesphant, R.; Penny, J.; Attwood, D.; McKeown, N. B.; D'Emanuele, A. Engineering of dendrimer surfaces to enhance transepithelial transport and reduce cytotoxicity. *Pharm. Res.* **2003**, *20* (10), 1543−50.
(37) Sweet, D. M.; Kolhatkar, R. B.; Ray, A.; Swaan, P.; Ghandehari, H. Transepithelial transport of PEGylated anionic poly(amidoamine) dendrimers: implications for oral drug delivery. *J. Controlled Release* **2009**, *138* (1), 78−85.
(38) Zhu, S.; Hong, M.; Tang, G.; Qian, L.; Lin, J.; Jiang, Y.; Pei, Y. Partly PEGylated polyamidoamine dendrimer for tumor-selective targeting of doxorubicin: the effects of PEGylation degree and drug conjugation style. *Biomaterials* **2010**, *31* (6), 1360−71.
(39) He, H.; Li, Y.; Jia, X.-R.; Du, J.; Ying, X.; Lu, W.-L.; Lou, J.-N.; Wei, Y. PEGylated poly(amidoamine) dendrimer-based dual-targeting carrier for treating brain tumors. *Biomaterials* **2010**, *32*, 478−487.
(40) Kannan, S.; Kolhe, P.; Raykova, V.; Glibatec, M.; Kannan, R. M.; Lieh-Lai, M.; Bassett, D. Dynamics of cellular entry and drug delivery by dendritic polymers into human lung epithelial carcinoma cells. *J. Biomate.r Sci. Polym. Ed.* **2004**, *15*, 311−330.
(41) Kitchens, K. M.; Ghandehari, H. PAMAM Dendrimers as Nanoscale Oral Drug Delivery Systems. In *Nanotechnology in Drug Delivery*; de Villiers, M. M., Aramwit, P., Kwon, G. S., Eds.; Springer Science: New York, 2009; Vol. *X*, pp 423−459.
(42) Saovapakhiran, A.; D'Emanuele, A.; Attwood, D.; Penny, J. Surface modification of PAMAM dendrimers modulates the mechanism of cellular internalization. *Bioconjugate Chem.* **2009**, *20* (4), 693−701.
(43) Mathias, N. R.; Timoszyk, J.; Stetsko, P. I.; Megill, J. R.; Smith, R. L.; Wall, D. A. Permeability characteristics of Calu-3 human bronchial epithelial cells: in vitro−in vivo correlation to predict lung absorption in rats. *J. Drug Target.* **2002**, *10*, 31−40.
(44) Linnankoski, J.; Makela, J.; Palmgren, J.; Mauriala, T.; Vedin, C.; Ungell, A. L.; Lazorova, L.; Artursson, P.; Urtti, A.; Yliperttula, M. Paracellular porosity and pore size of the human intestinal epithelium in tissue and cell culture models. *J. Pharm. Sci.* **2010**, *99* (4), 2166−75.
(45) Tajarobi, F.; El-Sayed, M.; Rege, B. D.; Polli, J. E.; Ghandehari, H. Transport of poly amidoamine dendrimers across Madin−Darby canine kidney cells. *Int. J. Pharm.* **2001**, *215* (1−2), 263−7.
(46) Buckley, S. T.; Kim, K.-J.; Ehrhardt, C. In Vitro Cell Culture Models for Evaluating Controlled Release Pulmonary Drug Delivery. In *Controlled Pulmonary Drug Delivery*; Smyth, H. D. C., Hickey, A. J., Eds.; Springer: New York, 2011; pp 417−442.
(47) Jain, K.; Kesharwani, P.; Gupta, U.; Jain, N. K. Dendrimer toxicity: let's meet the challenge. *Int. J. Pharm.* **2010**, *394*, 122−142.
(48) Wang, W.; Xiong, W.; Wan, J.; Xu, H.; Yang, X. The decrease of PAMAM dendrimer-induced cytotoxicity by PEGylation via attenuation of oxidative stress. *Nanotechnology* **2009**, *20*, 105−113.
(49) Qi, R.; Y, G.; Tang, Y.; He, R.-R.; Liu, T.-L.; He, Y.; Sun, S.; Li, B.-Y.; Li, Y.-B.; Liu, G. PEG-conjugated PAMAM dendrimers mediate efficient intramuscular gene expression. *AAPS J.* **2009**, *11*, 395−405.


DOI: 10.1021/mp500662z
*Mol. Pharmaceutics* 2015, 12, 826−838

(50) Forbes, B.; Ehrhardt, C. Human respiratory epithelial cell culture for drug delivery applications. *Eur. J. Pharm. Biopharm.* **2005**, *60* (2), 193−205.
(51) Haghi, M.; Young, P. M.; Traini, D.; Jaiswal, R.; Gong, J.; Bebawy, M. Time- and passage- dependent characteristics of a Calu-3 respiratory cell model. *Drug Dev. Ind. Pharm.* **2010**, *36*, 1207−1214.
(52) Vllasaliu, D.; Fowler, R.; Garnett, M.; Eaton, M.; Stolnik, S. Barrier characteristics of epithelial cultures modelling the airway and intestinal mucosa: a comparison. *Biochem. Biophys. Res. Commun.* **2011**, *415* (4), 579−85.
(53) Ong, H. X.; Traini, D.; Bebawy, M.; Young, P. M. Ciprofloxacin is actively transported across bronchial lung epithelial cells using a Calu-3 air interface cell model. *Antimicrob. Agents Chemother.* **2013**, *57* (6), 2535−40.
(54) Bi, X.; Shi, X.; Baker, J. R., Jr. Synthesis, characterization and stability of a luteinizing hormone-releasing hormone (LHRH)-functionalized poly(amidoamine) dendrimer conjugate. *J. Biomater. Sci. Polym. Ed.* **2008**, *19* (1), 131−42.
(55) Jevprasesphant, R.; Penny, J.; Attwood, D.; D'Emanuele, A. Transport of dendrimer nanocarriers through epithelial cells via the transcellular route. *J. Controlled Release* **2004**, *97* (2), 259−67.
(56) Navath, R. S.; Wang, B.; Kannan, S.; Romero, R.; Kannan, R. M. Stimuli-responsive star poly(ethylene glycol) drug conjugates for improved intracellular delivery of the drug in neuroinflammation. *J. Controlled Release* **2010**, *142* (3), 447−56.
(57) Yellepeddi, V. K.; Kumar, A.; Palakurthi, S. Biotinylated poly(amido)amine (PAMAM) dendrimers as carriers for drug delivery to ovarian cancer cells in vitro. *Anticancer Res.* **2009**, *29* (8), 2933−43.
(58) Mitragotri, S.; Lahann, J. Materials for drug delivery: innovative solutions to address complex biological hurdles. *Adv. Mater.* **2012**, *24* (28), 3717−3723.
(59) Kitchens, K. M.; Kolhatkar, R. B.; Swaan, P. W.; Eddington, N. D.; Ghandehari, H. Transport of poly(amidoamine) dendrimers across Caco-2 cell monolayers: Influence of size, charge and fluorescent labeling. *Pharm. Res.* **2006**, *23* (12), 2818−26.
(60) Pisal, D. S.; Yellepeddi, V. K.; Kumar, A.; Palakurthi, S. Transport of surface engineered polyamidoamine (PAMAM) dendrimers across IPEC-J2 cell monolayers. *Drug Delivery* **2008**, *15* (8), 515−22.
(61) Pisal, D. S.; Yellepeddi, V. K.; Kumar, A.; Kaushik, R. S.; Hildreth, M. B.; Guan, X.; Palakurthi, S. Permeability of surface-modified polyamidoamine (PAMAM) dendrimers across Caco-2 cell monolayers. *Int. J. Pharm.* **2008**, *350* (1−2), 113−21.
(62) Anderson, J. M. Molecular structure of tight junctions and their role in epithelial transport. *Physiology* **2001**, *16*, 126−130.
(63) Casettari, L.; Vllasaliu, D.; Mantovani, G.; Howdle, S. M.; Stolnik, S.; Illum, L. Effect of PEGylation on the toxicity and permeability enhancement of chitosan. *Biomacromolecules* **2010**, *11*, 2854−2865.
(64) Lai, S. K.; O'Hanlon, D. E.; Harrold, S.; Man, S. T.; Wang, Y. Y.; Cone, R.; Hanes, J. Rapid transport of large polymeric nanoparticles in fresh undiluted human mucus. *Proc. Natl. Acad. Sci. U.S.A.* **2007**, *104* (5), 1482−7.
(65) Wang, Y. Y.; Lai, S. K.; Suk, J. S.; Pace, A.; Cone, R.; Hanes, J. Addressing the PEG mucoadhesivity paradox to engineer nanoparticles that "slip" through the human mucus barrier. *Angew. Chem., Int. Ed.* **2008**, *47* (50), 9726−9.
(66) Bucior, I.; Mostov, K.; Engel, J. N. *Pseudomonas aeruginosa*-mediated damage requires distinct receptors at the apical and basolateral surfaces of the polarized epithelium. *Infect. Immun.* **2010**, *78* (3), 939−53.
(67) Goldberg, D. S.; Ghandehari, H.; Swaan, P. W. Cellular entry of G3.5 poly (amido amine) dendrimers by clathrin- and dynamin-dependent endocytosis promotes tight junctional opening in intestinal epithelia. *Pharm. Res.* **2010**, *27* (8), 1547−57.
(68) Plotkowski, M. C.; Costa, A. O.; Morandi, V.; Barbosa, H. S.; Nader, H. B.; de Bentzmann, S.; Puchelle, E. Role of heparan sulphate proteoglycans as potential receptors for non-piliated *Pseudomonas aeruginosa* adherence to non-polarised airway epithelial cells. *J. Med. Microbiol.* **2001**, *50* (2), 183−90.
(69) Longmire, M.; Choyke, P. L.; Kobayashi, H. Clearance properties of nano-sized particles and molecules as imaging agents: considerations and caveats. *Nanomedicine* **2008**, 3 (5), 703−17.
(70) Ryan, G. M.; Kaminskas, L. M.; Kelly, B. D.; Owen, D. J.; McIntosh, M. P.; Porter, C. J. Pulmonary administration of PEGylated polylysine dendrimers: absorption from the lung versus retention within the lung is highly size-dependent. *Mol. Pharmaceutics* **2013**, *10* (8), 2986−95.


DOI: 10.1021/mp500662z
*Mol. Pharmaceutics* 2015, 12, 826−838